The Abdus Salam
International Centre
for Theoretical Physics

United Nations
Educational, Scientific and
Cultural Organization

IAEA
International Atomic Energy Agency

2484-7

ICTP-IAEA Joint Workshop on Nuclear Data for Science and Technology: Medical Applications

30 September - 4 October, 2013

Statistical theory of nuclear reactions

A.V. Ignatyuk
Institute of Physics and Power Engineering
Obninsk
Russia

Statistical theory of nuclear reactions

A.V.Ignatyuk,
Institute of Physics and Power Engineering, Obninsk, Russia

Theoretical models of nuclear processes play an important role in all stages of nuclear data evaluation for both a general understanding of the physical phenomena related to the analyzed data and to estimate the required cross-sections in cases where data are contradictive or not fully available. A brief description is given of the models and codes used in practical evaluations. All employed nuclear reaction codes are based on rather similar models of nuclear processes, but differ essentially in their detail and input parameters. Main differences between the calculated cross-sections are discussed for some reactions important for medical applications.

1. NUCLEAR REACTION MODELS

Nuclear reaction theory is based, to a significant extent, on the compound nucleus model proposed by Bohr more than seventy years ago [1]. A nuclear reaction can be considered as proceeding in two stages: the formation of the compound nucleus by the collision of a projectile with a target nucleus and the decay of the resulting compound nucleus into pairs of reaction products. The corresponding reaction cross-section can be expressed by the following equation:

$$\sigma(a,b) = \sigma_c(a) P_b / \sum_{b'} P_{b'} \quad , \tag{1}$$

where $\sigma_c(a)$ is the cross section for the compound nucleus formed by projectile *a,* and P_b is the probability of the compound nucleus decaying into the corresponding outgoing channel *b*. The denominator of Eq. (1) includes the sum over all possible decay channels. The decay probability of the compound nucleus can be given in the form:

$$P_b(e_b) = \frac{g_b \mu_b e_b \sigma_c^*(e_b)}{\pi^2 \hbar^3} \frac{\rho_b(U_b)}{\rho_c(U_c)} \quad , \tag{2}$$

where e_b is the energy of the emitted particle, $g_b = 2s_b+1$ is the statistical factor connected with the spin s_b of the particle, μ_b is the reduce mass, $\sigma_c^*(e_b)$ is the cross section for the inverse reaction, and ρ_b and ρ_c are the level densities for the residual and compound nucleus at the corresponding excitation energies. All component energies are connected by the relationship $U_c=U_b+B_b+e_b$, where B_b is the binding energy of the particle in the compound nucleus. The sum of the decay probabilities over all channels including the integrals over energies of emitted particles determines directly the inverse value of the average lifetime of the compound nucleus with the given excitation energy.

Eq. (2) demonstrates the evident statistical form of the nuclear reaction description. All specific features of the dynamics of the nuclear process are related to the inverse reaction cross-section, while other components estimate the phase space accessible for the reaction products. Such a description is very similar to those for the particle evaporation from a liquid surface, and, for this reason, the above equation is referred to as the evaporation model or Weisskopf-Ewing formula [2].

A more rigorous consideration of the nuclear process defines compound reaction cross-sections in terms of the Hauser-Feshbach-Moldauer formula [3-5]:

$$\sigma(a,b) = \pi \lambda\!\!\!^{-2}_a \sum_{J\pi} g_s^J \frac{T_a^{J\pi} T_b^{J\pi}}{\sum_c T_c^{J\pi}} F_{ab,c}^{J\pi}, \tag{3}$$

where $\lambda\!\!\!^{-}_a$ is the wave length of the incident particle, $T_a^{J\pi}$ are the transmission coefficients for the given angular momentum J and parity π, and $F_{ab,c}$ is the width fluctuation correction for differences between the averaged ratio of fluctuating decay widths and the ratio of the averaged widths [5]. This correction is only important for low energies of incident particles when the number of open reaction channels is rather small.

For a large number of channels the sum of the transmission coefficients in the numerator and denominator of Eq. (3) should be replaced by integrals of the form:

$$\sum_c T_c = \sum_{l,j,I} \int_0^{U_{\max}} T_{lj}(E_c)\rho(U,I)dU \ , \qquad (4)$$

which contain the level densities of the residual nuclei. The sum in Eq. (4) is taken over all combinations of the angular momentums and spins of the reaction products, including the given quantum characteristics of the compound nucleus. With an increase in the number of channels, the level density plays an increasingly important role in the correct description of reaction cross sections that pass through the compound nucleus stage.

The transmission coefficients are usually calculated by means of the optical model [4] and such an approach has been used successfully by many authors to describe a large amount of experimental data on neutron-induced reaction cross-sections at energies below 10 MeV. At higher energies, the influence of the angular-momentum conservation law on the selection of reaction channels decreases particularly for the light-particle reactions, and the descriptions of reaction cross-sections on the basis of the evaporation model (2) and the more rigorous formulae (3) become very similar.

For the neutron radiative capture the Hauser-Feshbach-Moldauer relation (3) can be written in the form

$$\sigma_{n\gamma} = \pi\lambda\!\!\!^{-2}_n \sum_{J,l,j} g_J T^{J\pi}_{lj}(E_n) \frac{T^{J\pi}_{\gamma c}(E_n) F^{J\pi}_{lj\gamma}(E_n)}{T^{J\pi}_{\gamma}(E_n) + \sum_{n'l'j'} T^{J\pi}_{l'j'}(E_{n'})} \qquad (5)$$

were T_γ are the radiative transmission coefficients connected with the radiative widths through the relation

$$T^{J\pi}_{\gamma}(E_n) = 2\pi\Gamma^{J\pi}_{\gamma}(B_n + E_n) / D^{J\pi}(B_n + E_n) \qquad (6)$$

Because the excitation energy of a residual nucleus after the emission of low-energy gamma-quanta can be above the neutron binding energy and the reactions of (n,γn′),…, (n,xγn′) can be possible, the numerator of Eq. (5) includes only the capture radiative coefficients corresponding to the reaction channels without the secondary emission of neutrons.

The available experimental data on the radiative capture of fast neutrons have been analysed by many authors and nowadays the corresponding calculations can be performed rather simply with the codes considered later.

An effect of different factors on the calculated cross sections can be traced in Fig. 1, where the statistical model calculations are compared with the experimental data for the ^{68}Zn(n,γ) reaction. Contributions of the various partial waves change rather quickly with the increasing of a neutron energy and the relative contributions depend essentially on the corresponding neutron strength functions. For the neutron energies below the first excited level of the taget nucleus the fluctuation correction (2.24) reduces the calculated cross section by 15-25%. For higher energies, when several inelastic scattering channels are open, the fluctuation corrections lead to a redistribution of partial wave contributions on account of which the total capture cross section can even increase. With the subsequent increase of a number of open inelastic channels the effects of fluctuation corrections disappear rather quickly. On the other hand the energy dependence of the radiative strengths functions and the nuclear level densities begins to effect increasingly on the calculated results with a growth of the incident neutron energy.

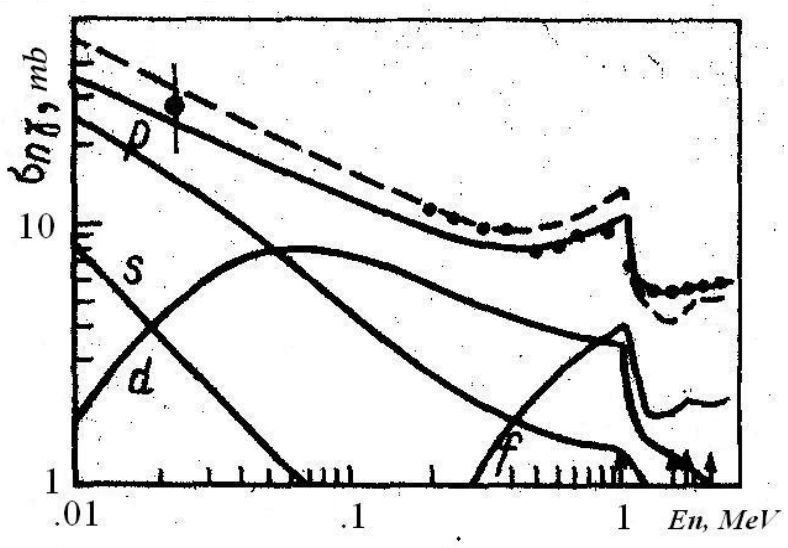

Fig. 1. Neutron capture cross sections for ^{68}Zn, calculated taking into account the width-fluctuation corrections (solid curves) and without such corrections (dashed curve). The contributions of various partial waves are shown together with the corresponding experimental data for the total capture cross section (black symbols).

An increase of projectile energy above several MeV increases the probability that the projectile or some products of the intranuclear collisions escape from the nucleus before the compound nucleus stage considered above. Such occurrences are usually referred to as pre-compound or pre-equilibrium processes. The simplest correspond to the first projectile collisions or excitation of low-lying collective nuclear levels, and are defined as direct reactions that have been well developed as the Distorted Wave Born Approximation (DWBA) or the Coupled-Channels (CC) approaches [6, 7].

Nucleon emission from more complex pre-equilibrium transitions has been considered by adopting the exciton model [8] as proposed by Griffin. The intermediate states of the excited nucleus in this model can be classified by the number of excited particles and holes or quasi-particles ($n=p+h$), and the emission of nucleons from each intermediate state can be described by equations, which differ from those of the evaporation model (1) and (2) through the explicit definition of n-exciton states:

$$P_n(e_b) = \frac{g_b \mu_b e_b \sigma_c^*(e_b)}{\pi^2 \hbar^3} \frac{\rho_{n-1}(U_b)}{\rho_n(U_c)} \ , \tag{7}$$

where $\rho_n(U)$ are the densities of the corresponding states with a given excitation energy. The total probability of the preequilibrium nucleon emission can be obtained as the sum over all preequilibrium states for the product of Eq. (5) and the average lifetime of the n-exciton states τ_n. This lifetime can be estimated as the inverse of the transition rate from n-exciton states to more complex n+2-exciton states, and can be written as the equation:

$$\tau_n^{-1}(U_c) \approx \lambda_{n \to n+2} = \frac{2\pi}{\hbar} |M|^2 \rho_{n,f}(U_c) \ , \tag{8}$$

where |M| is the averaged matrix element for the corresponding transitions, and $\rho_{n,f}$ is the density of the corresponding final states [9].

Various modifications of the preequilibrium model were proposed in Refs. [10-16]. These publications include more detailed discussions of the corresponding relationships for the level densities and transition rates, as well as examples of applications of such models to the analysis of numerous experimental data. A more substantial list of references and applications can be found in the monograph on pre-equilibrium nuclear reactions [17].

Combined pre-equilibrium plus compound models have been incorporated into many computer codes, the most popular of which are ALICE, GNASH, and the recently released EMPIRE and TALYS codes. All of these codes were used to calculate the reaction cross-sections interesting for various medical applications [18]. We will discuss the main features of these codes, which are important in understanding the divergences between calculations, and represent a means of estimating the uncertainties of such calculations.

2. NUCLEAR LEVEL DENSITY

An essential part of our current knowledge on nuclear structure has obtained from investigations of the low-lying nuclear levels. However, a number of levels for medium and heavy nuclei grow so rapidly with increasing excitation energy that the spectroscopic analysis for each level becomes practically unfeasible. In such conditions a transition to the statistical description of nuclear properties looks natural and quite reasonable. The nuclear level density is the most important statistical characteristics of excited nuclei.

Simple analytical relations for the state density $\omega(U)$ of a nucleus with a given excitation energy U and the level density $\rho(U,J)$ of a nucleus with a given angular momentum J have been obtained by Bethe on the basis of the Fermi gas model [19]:

$$\begin{aligned} \omega(U) &= \frac{\sqrt{\pi}}{12 a^{1/4} U^{5/4}} \exp\left(2\sqrt{aU}\right) \\ \rho(U,J) &= \frac{2J+1}{2\sqrt{2\pi}\sigma^3} \omega(U) \exp\left[-\frac{(J+1/2)^2}{2\sigma^2} \right] \end{aligned} \tag{9}$$

Here $a = \pi^2 g/6$ is the level density parameter, which is proportional to the single-particle state density g near the Fermi energy, and σ^2 is the spin cutoff parameter.

For the Fermi gas model the state equations determining a dependence of the excitation energy U, the entropy S and other thermodynamic functions of a nucleus on its temperature t have a simple form:

$$U = at^2 \ , \qquad S = 2at \ , \qquad \sigma^2 = \langle m^2 \rangle gt \ , \tag{10}$$

where $<m^2>$ is the mean square value of the angular momentum projections for the single-particle states around the Fermi energy, which may also be associated with the moment of inertia of a heated nucleus $\Im = g<m^2>$. The connection of the thermodynamic functions (10) with the state and level densities (9) is obvious.

The main parameters of the Fermi-gas model may be estimated rather simply using the semiclassical approximation:

$$a = 2\left(\frac{\pi}{3}\right)^{4/3} \frac{m_o r_o^2}{\hbar^2} A\left(1 + b_s A^{-1/3}\right), \quad \Im_0 = \frac{2}{5}\frac{m_0 r_0^2}{\hbar^2} A^{5/3} \tag{11}$$

where m_0 is the nucleon mass, r_0 is the radial parameter, A is the mass number and b_s defines the surface component of the single-particle level density.

The most direct information on the level density of highly excited nuclei is obtained from the average parameters of neutron resonances. For the majority of nuclei the observed resonances correspond to s-neutrons, therefore the value of D_0 is related to the level density of the compound nucleus by the relations:

$$D_0^{-1} = \begin{cases} \frac{1}{2}\left\{\rho(B_n + \Delta E/2, I_0 + 1/2) + \rho(B_n + \Delta E/2, I_0 - 1/2)\right\} & for\ I_0 \neq 0 \\ \frac{1}{2}\rho(B_n + \Delta E/2, 1/2) & for\ I_0 = 0 \end{cases}, \tag{12}$$

were B_n is the neutron binding energy, ΔE is the energy interval for which the resonances are being examined, I_0 is the target nucleus spin, and the coefficient 1/2 before the sum takes into account the fact that s-neutrons form resonances only of a particular parity. If necessary, resonances for *p*-neutrons can be taken into consideration analogously.

The experimental values of D_s are normally used as source data, from which the magnitude of the level density parameter can be derived by means of Eqs. (9) and (12). Many authors have carried out such an analysis and its recent results are collected in the RIPL-3 library together with the references to previous publications [20].

The regular differences of the level densities for even-even, odd and even-odd nuclei analogous to the even-odd differences of the nuclear masses have been already noted on the first systematics of experimental data. To take this effect into account it is usual to introduce the so-called effective excitation energy defined as

$$U^* = U - \begin{cases} \delta_Z + \delta_N \text{ for even - even} \\ \delta_Z \textit{ for } \text{even Z} \\ \delta_N \text{ for even N} \\ 0 \textit{ for } \text{odd - odd} \end{cases} \tag{13}$$

where δ_I is the corresponding phenomenological correction for even-odd differences of the nuclear binding energies.

The level density parameters obtained in the framework of such an approach are shown in the upper part of Fig. 2. The values of a -parameters differ greatly from the semi-classical estimation (11). In the lower part of this figure the shell corrections to the nuclear mass formula are shown which are determined as

$$\delta E_0 = M_{\exp}(Z, A) - M_{ld}(Z, A, \beta), \tag{14}$$

where M_{exp} is the experimental value of the mass defect and M_{ld} is the liquid drop component of the mass formula calculated for the equilibrium nuclear deformations β [21]. The strong correlation of the shell corrections and the ratio a/A should be considered as a direct evidence of the important role of shell effects in the description of level densities and other statistical characteristics of excited nuclei.

Data on the cumulative numbers of low-lying nuclear levels are also very important for the level density analysis. Many years ago it has been noted [22] that the observed energy dependence of the cumulative number of levels is described rather well by the function

$$N(U) = \exp\left[(U - U_0)/T\right], \tag{15}$$

where U_0 and T are free parameters determined by the fitting to corresponding data. The quantity $N(U)$ is related to the level density by the relation

$$\rho_{lev}(U) = \frac{dN}{dU} = \frac{1}{T}\exp\left[(U - U_0)/T\right], \tag{16}$$

and it is obvious that the parameter T corresponds simply to a nuclear temperature. Since the value of this parameter is assumed to be constant over the energy range considered, Eq. (16) are called the constant temperature model.

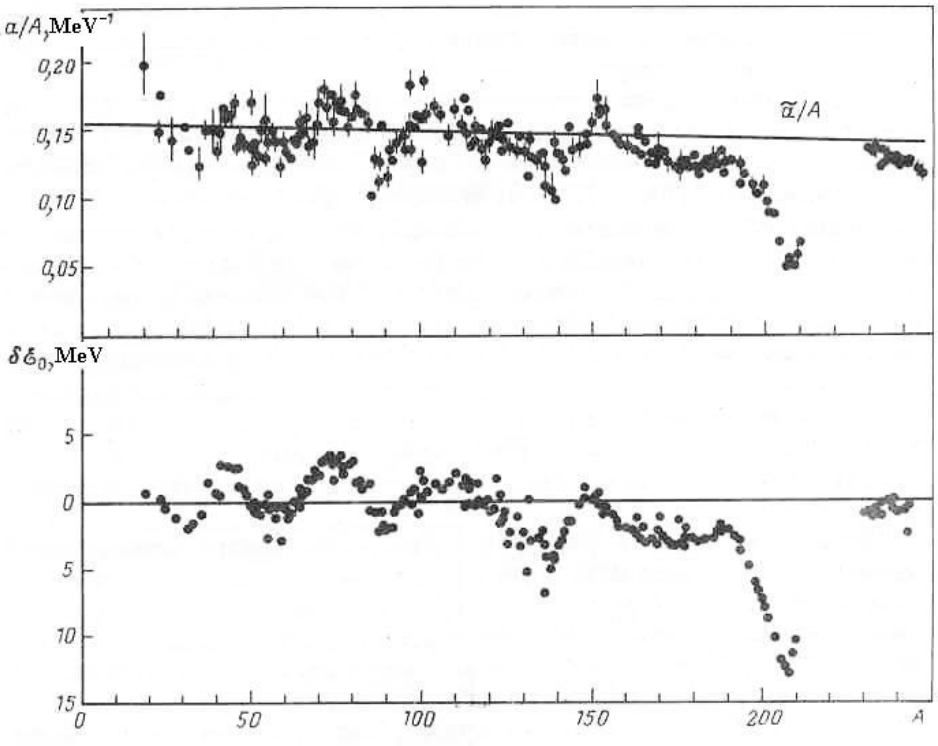

Fig. 2. Ratio of the Fermi-gas level density parameter to the mass number (upper plot) and the shell corrections to the nuclear mass formula (bottom plot)

To obtain the level density for the whole range of excitation energies, Gilbert and Cameron [23] proposed to combine the low-energy region (16) with the high-energy dependence predicted by the previously described Fermi gas model. Such an approach is usually called the Composite Gilbert-Cameron model. The link between both models' parameters can be found from the condition of continuity for the level density and its first derivative at some matching energy

$$U_x = U_0 + T\ln\left[T\rho_{fg}(U_x)\right] \quad , \qquad \frac{1}{T} = \sqrt{\frac{a}{U_x^*}} - \frac{3}{2U_x^*} \quad , \tag{17}$$

where U_x^* is the effective matching energy that includes the even-odd corrections (13).

The recent results of experimental data analysis in the framework of this phenomenological approach are presented in the RIPL-3 library and the obtained parameters are shown in Fig. 3. The values of U_x determine the energies below which the level density description in terms of the Fermi-gas model becomes unsatisfactory, and one can see that for the majority of nuclei this energy is rather high.

Another approach to the problem of simultaneous description of neutron resonance densities and low-lying levels was proposed in Ref. [24]. It has been assumed that both sets of experimental data can be described on the basis of the Fermi-gas relations, if the level density parameter a and the excitation energy shift δ_{eff} are considered as free parameters for each nucleus. Since for odd-odd nuclei the displacement thus found is negative, the above approach has been called as the back-shifted Fermi-gas model. All data available on the neutron resonance densities and low-lying nuclear levels were analyzed, and parameters a and δ_{eff} have been estimated for the entire mass region. Due to another determination of effective excitation energies the values obtained for the a-parameter are naturally somewhat lower then those shown in Fig. 2. However, the shell effects in the mass dependence of a-parameters remain essentially invariable.

The results of all consistent microscopic calculations of the nuclear level densities display the damping of the shell effect at high excitation energies. To include the shell effect damping into consideration the level density parameters should be energy dependent. This dependence may be approximated by the formula [25]

$$a(U,Z,A) = a_{as}(A)\left\{1 + \frac{\delta E_0}{U}\left[1 - \exp(-\gamma U)\right]\right\} \quad , \tag{18}$$

where a_{as} is the asymptotic level density parameter to which $a(U)$ tends for high excitation energies and γ is the damping parameter. From a fit of a-parameters with the Myers-Swiatecki shell corrections the following coefficients (in MeV^{-1}) have been obtained: $a_{as} = 0.0959A+0.1468A^{2/3}$, $\gamma=0.325/A^{1/3}$.

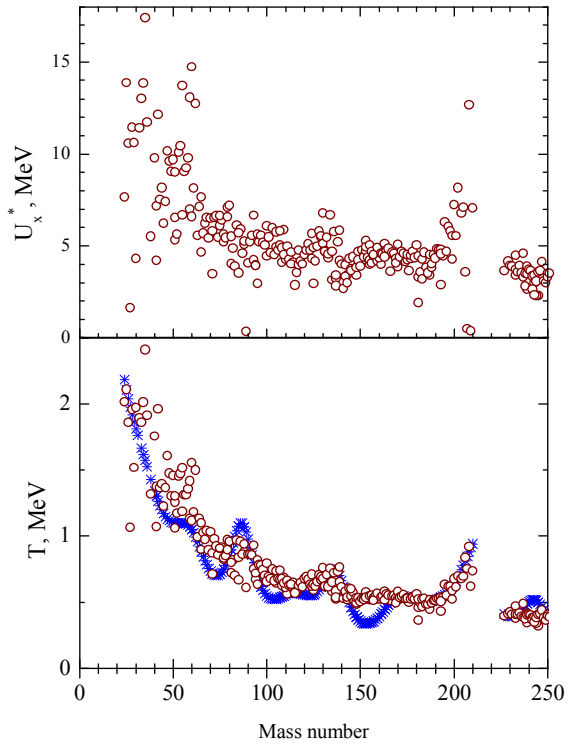

Fig. 3. Mass-number dependence on the nuclear temperature T and the effective excitation energy U_x, bellow of which the level density approximated with the constant temperature model. Blue crosses show the results of the independent analysis of the low-lying discrete levels.

The systematics based on the similar formulas have been discussed by many authors and main differences between the obtained parameters relate to estimations of the shell corrections. More detailed discussion of such parameters in the RIPL-3 description [20].

On the basis of above results we can conclude that the Fermi-gas and constant temperature models provide us with comparatively simple and convenient formulas for parametrizing experimental data on nuclear level densities. However, these models do not give any explanation for the shifts of excitation energies and shell changes of the level density parameters. An interpretation of these effects must be obtained on the basis of more rigorous models that take into consideration shell inhomogenities of single-particle level spectra, on the one hand, and the superfluid and collective effects produced by the residual interaction of nucleons, on the other. A detailed discussion of such models can be found in the monograph [26]. However, rigorous microscopic methods of level density calculations are extremely laborious and this severely limits their application to experimental data analysis. For this reason there is a need to have the level density description, that take into account the basic ideas of microscopic approaches concerning the structure of highly excited nuclear levels while being sufficiently simple and convenient for broad application.

The level density calculations discussed above are based on a consideration of the total energy of an excited nucleus as the sum over all possible combinations of quasi-particle energies. If we include into these combinations all possible rotational or vibrational excitations then the level density of a excited nucleus may be written in the form

$$\rho(U) = \rho_{qp}(U)K_{vibr}K_{rot} \quad , \tag{19}$$

where ρ_{qp} is the level density due to quasi-particle excitations only, and K_{vibr} and K_{rot} are the corresponding enhancement coefficients.

In adiabatic approximation the rotational enhancement of the level density depends from the nuclear shape symmetry and can be written as [27]:

$$K_{rot} = \begin{cases} 1 & \text{for spherical nuclei,} \\ \Im_{\perp} t & \text{for deformed nuclei,} \end{cases} \tag{20}$$

where $\Im_i$ is the moment of inertia relatively to the perpendicular axis. This formula is obtained on the assumption of the mirror and axial symmetry of deformed nuclei. This shape have most stable nuclei of the rare-earth elements ($150 \le A \le 190$) and the actinides $A \ge 230$. For non-axial forms the rotational enhancement of the level density becomes even greater [27].

The vibrational enhancement coefficient is determined in the microscopic approach by the relation

$$K_{vibr} = \prod_i \left[\frac{1-\exp\left(-\omega_i^0 / t\right)}{1-\exp\left(-\omega_i / t\right)} \right]^{g_i} , \qquad (21)$$

where ω_j is the energy of vibrational excitations, ω_i^o is the energies of corresponding quasi-particle excitation and g_i is the degeneracy of such excitations. The presence of quasi-particle energies in Eq. (21) reflects some account of non-adiabatic effects in excited nuclei. Due to the symmetry conditions imposed on the nuclear Hamiltonian the rotational and vibrational excitations become connected by some relations in consistent microscopic approach [26]. As a result the calculated collective enhancement coefficients turn out always reduced in comparison to the adiabatic estimation.

It can readily be seen that the adiabatic estimation of K_{rot} increases the nuclear level densities by a factor of 50-100 compared to the calculations based on quasi-particle excitations alone. The increase of the level density due to vibrational excitations will be appreciable only for low-energy excitations with ω_i < 1-2 MeV.

The influence of pairing correlations of superconductive type on nuclear properties can be characterized by the correlation functions $\Delta_{o\tau}$, which directly determine the even-odd differences in the nuclear binding energies and the energy gap $2\Delta_{o\tau}$ in the spectrum of quasi-particle excitations of even–even nuclei. The critical temperature t_{cr} of the phase transition from a superfluid to a normal state is connected with the correlation function through the relation

$$t_c = 0.567\Delta_0 . \qquad (22)$$

The excitation energy corresponding to the critical temperature may be written as:

$$U_{cr} = 0.472 a_{cr}\Delta_0^2 - n\Delta_0 , \qquad (23)$$

where n = 0, 1 and 2 for even-even, odd and odd–odd nuclei, respectively. Above the critical energy the level density and other nuclear thermodynamic functions can be described by the Fermi gas relations, in which the effective excitation energy is defined as

$$U^* = U - E_{cond} . \qquad (24)$$

Here E_{cond} is the condensation energy that determines a reduction of the nuclear ground state energy due to the pairing correlations:

$$E_{cond} = 0.152 a_{cr}\Delta_0^2 - n\Delta_0 . \qquad (25)$$

To take into account the shell effects the energy dependence of the level density parameter should be modified in the corresponding way:

$$a(U,Z,A) = \begin{cases} \tilde{a}(A)\left\{1 + \delta E_0 \dfrac{f(U^*)}{U^*}\right\} \text{ for U} \geq U_{cr} \\ a_{cr}(U_{cr},Z,A) \; for \; U < U_{cr} \end{cases} \qquad (26)$$

Below the phase-transition point (23) the expressions for thermodynamic functions of a nucleus are rather complex, and they will not be considered here. The complete expressions can be found in Refs. [26]. The differences between the thermodynamic functions of the superfluid model and Fermi-gas model are shown in Fig. 4. The differences are most remarkable for the moments of inertia, and available experimental data about the temperature dependence of the effective moments of inertia for fissioning nuclei give the best evidence for the existence of the corresponding phase transition in excited nuclei [26].

Eq. (26) was used as the basic one to construct a phenomenological version of the generalized superfluid model (GSM). Applying above relations for a description of the pairing correlation effects the level density enhancement coefficients were estimated from the experimental data on the densities of neutron resonances. In such analysis the asymptotic values of the level density parameters were defined as a_{as} = 0.073 A + 0.115 $A^{2/3}$ MeV , the shell corrections were taken from Ref. [21] and the correlation functions approximated as Δ_o = $12/A^{1/2}$ MeV. The coefficients obtained are shown in the upper part of Fig. 5. In the lower part the values of similar coefficients calculated in the adiabatic approximation are given. A correlation of both coefficients is very strong but as a rule the adiabatic evaluations give higher values of coefficients than the similar ones extracted from the observed density of neutron resonances. The difference of these two definitions of the level density enhancement factors demonstrates that the damping of the enhancement coefficients for highly excited nuclei should be taken into account.

At first glance it might seem that the systematics of the level density parameters in terms of the Fermi gas and the GSFM are equally justified, since they give approximately identical description of the level densities

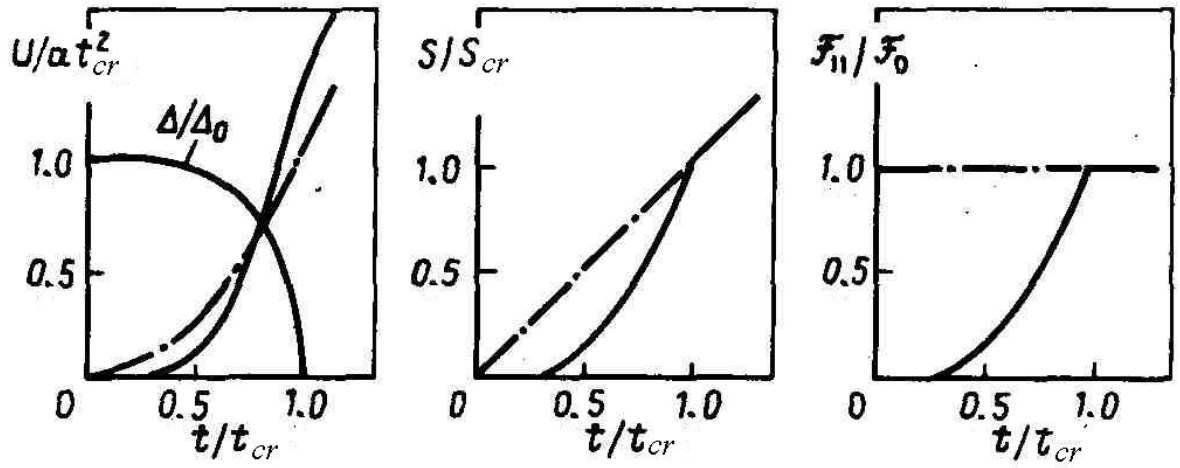

Fig. 4. Temperature dependence of the nuclear thermodynamic functions for the superfluid model (solid lines) and the Fermi-gas model (dashed-dotted corves)

at excitation energies close to the neutron binding energy. However, these descriptions correspond to deferent absolute values of the level density parameters, because the inclusion of collective effects decreases the *a*-parameters obtained. These reduced values agree well enough with both the experimental data derived from the spectra of scattered neutrons with energies of up to **7** MeV and the theoretical calculations of the *a*-parameters for the single-particle level schemes of a Woods-Saxon potential [26]. This agreement of the data is very important, because the evaporation spectra are sensitive precisely to the value of the level density parameter rather than to the magnitude of the excited level density. It is impossible to explain differences between the values of *a*-parameter obtained from resonance data and from evaporation spectra in terms of the Fermi-gas model without account of collective effects. Proper consideration of the level density collective enhancement is also very important for a consistent description of the observed fissilities of highly-excited nuclei [26].

Today it seems almost obvious that in description of the level densities of excited nuclei we should to use the models, which are more consistent than the Fermi-gas, but inevitably more complex. The success of the generalized superfluid model is attributed to the inclusion of the main well-known component of nuclear theory: the pairing correlations, shell effects and collective excitations. Some complexity of the model seems

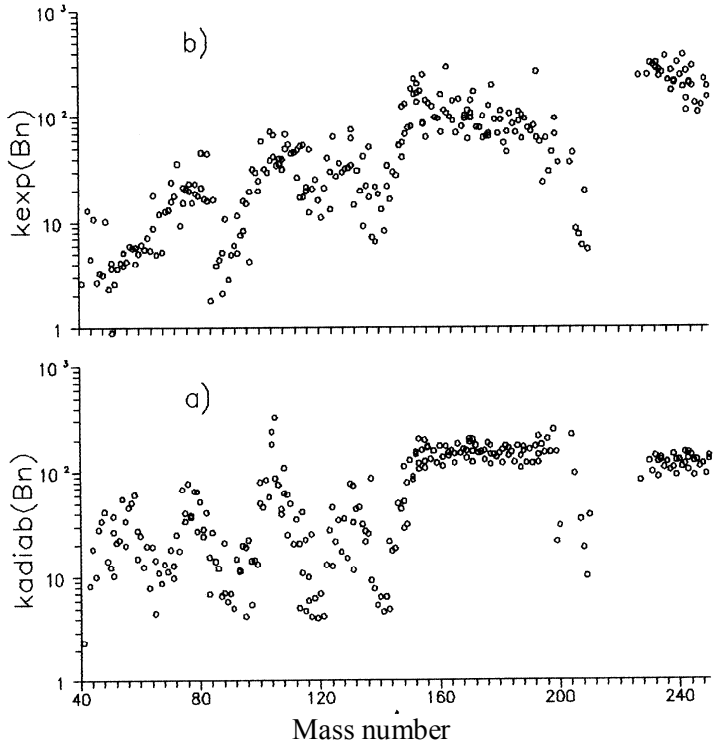

Fig. 5. Collective enhancement factors calculated in the adiabatic approximation (a) and obtained as the ratio of the observed density of neutron resonances to the calculated density of quasi-particle excitations (b).

to be justified by the mutual consistency of the parameters obtained from the various experimental data and also by the close relation of the theoretical concepts used to describe the structure of low-lying nuclear levels and the statistical properties of highly excited nuclei.
More detailed discussion of various versions of GSFM together with the corresponding parameters can be found in the RIPL-3 description [20].

3. OPTICAL MODEL

Indications of the significant transparency of nuclei were first obtained from the analysis of the neutron scattering cross sections with the energy of 90 MeV [28]. In order to describe the observed total and absorption cross sections a complex single-particle potential was used. Its real part corresponds to the mean field of a nucleus while the imaginary part determines the overall effect of all inelastic processes that remove the particle from the elastic channel. The relation between the imaginary part of the potential and the nuclear absorption coefficient was obtained from the consideration of the particle flux attenuation.
A further developments of the optical model was stimulated by the experiments on the scattering of neutrons with energies of several MeV conducted by Barshall [29]. Wide maxima were observed in the energy dependence of the neutron total cross sections, the positions of which changed smoothly with the mass number. Later similar maxima were observed in the differential neutron scattering cross sections as well. Feshbach, Porter and Weiskopf [30] demonstrated that common features of the observed cross sections can be reproduced within the optical model with the potential in the form of a complex square-well with the depth of 42(1 + 0.03i) MeV and radius $R_o = 1.45\ A^{1/3}$ fm. The imaginary potential value corresponds to the mean free path of 15-20 fm, which significantly exceeds the size of a nucleus. Thus nuclei are rather transparent for low-energy particles and this property plays an important role in the analysis of nuclear reactions.
Though the square well model describes the basic features of the irregular behaviour of the strength functions and the corresponding scattering cross sections, it is certainly too simplified to quantitatively describe experimental data. Therefore further development of the optical model proceeded by making the single-particle potential used more precise and complicated. At present this potential usually takes the form

$$V(r) = -(V_v + iW_v) f_v(r) + 4iW_s a_s \frac{df_s}{dr} + V_{so} \frac{\lambda\!\!\!^{-2}_{\pi}}{r} \frac{df_{so}}{dr} (\mathbf{l} \cdot \mathbf{s}) \quad , \qquad (27)$$

where $f_i(r) = [1 + \exp(\frac{r - R_i}{a_i})]^{-1}$ are the form-factors of the volume, surface and spin-orbital components of the optical potential, respectively, and the geometric parameters of the corresponding form-factors can be different in the general case.
Many authors attempted to find a universal set of optical potential parameters, which would give rather good description of a wide range of experimental data. At the same time they tried to keep the same geometrical parameters of the potential as in the shell model. They also take into consideration the dependence of the real and imaginary optical potential components on both the projectile energy and target isospin. Despite the large number of the parameters included in the analysis, calculations with universal sets of potential parameters reproduce correctly only the general trends of the cross section dependencies on the energy and nuclear mass number. To describe the cross sections in a particular nucleus a certain adjustment of the potential parameters is usually needed, especially when cross sections are related to the low-energy region. The strength functions of the *s*- and *p*-wave neutrons shown in Fig. 6 can serve as an example of the results obtained within the optical model calculations [31]. The calculations performed for some universal set of optical potential parameters do not reproduce the isotopic changes of the strength functions observed in the range of strength function minima. Neither does it show the splitting of *s*-wave strength functions in the rare-earth nuclei. For a more accurate description of the available data we should not limit ourselves to the one-channel optical model and include some additional structural effects.
In the one-channel model the influence of all possible reaction channels on the elastic scattering channel is approximated by means of the imaginary part of the optical potential. If the effect of some reaction channels is much stronger than that of others, as we observe, for example, for the inelastic scattering of nucleons on the low-lying collective levels, the generalized optical model or the of coupled channels method (CCM) [7, 32]

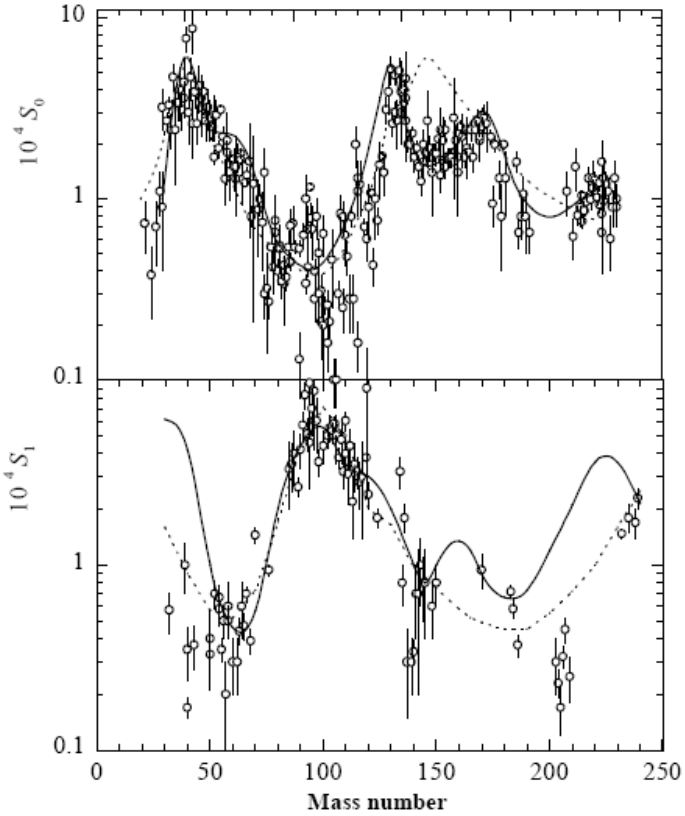

Fig. 6. Strength functions of *s*- and *p*-wave neutrons as a function of the mass number. Results of calculations are shown by dashed curves for the spherical optical model and solid ones for CCM.

should be used instead of the one-channel model. Within the phenomenological version of CCM the interaction between the neutron and the nucleus is described by the deformed optical potential

$$V(\mathrm{r}) = V(r) + V_{coupl}(r,\theta,\varphi) \quad , \tag{28}$$

where $V(r)$ is the spherical part of the potential similar to (27) and V_{couple} is the potential component responsible for the coupling of different reaction channels. V_{couple} can be expressed through the deformation parameters that describe the rotational or vibrational nuclear excitations. The coupling of the elastic scattering channel and those of closed inelastic scattering channels corresponding to low- lying collective levels is directly responsible for the splitting of the 3*s*-giant resonance of the neutron strength functions shown in Fig. 6. The coupling with the inelastic scattering channels is also important for the explanation of the isotopic dependence of the neutron strength functions.

Nowadays CCM is extensively used in the neutron cross-section analysis and numerous examples of experimental data descriptions obtained can be found in Refs. [7, 32]. The optical potential parameters obtained on the basis of the CCM analysis demonstrate a much smaller fluctuation from nucleus to nucleus than the individual sets of spherical optical model parameters. Besides, the parameters of the real component of the optical potentials are also in a much better agreement with the standard parameters of the shell model single-particle potential. This agreement is an important advantage of the generalized optical model. Practical recommendations on the optical potential parameters for individual nuclei are compiled in the RIPL-3 library [20].

When the mean free path is long, the probability of one of the particles escaping from the nucleus after one or several collisions of the projectile with a nucleon of the target nucleus is rather high. Such processes are usually referred to as direct nuclear reactions. A typical time of direct reactions is approximately the same as the transit time of a projectile $\sim 10^{-22}$ s and is much shorter than the time-life of a compound nucleus $\tau_c = 10^{-16}..10^{-19}$ s. As the number of intranuclear collisions is small, they cannot sufficiently disorient the

projectile, thus the particle escaping from the nucleus is usually concentrated in the front hemisphere. This asymmetrical character of the angular distribution of particles is a major characteristic of direct mechanisms of nuclear reactions.

The above time estimates show that direct transitions and comparatively slow processes in the stage of the quasi-equilibrium compound nucleus correspond to two extremes in the time scale of nuclear reaction evolution. It is natural to expect that the processes relevant to the intermediate transition stage between the fast direct and slow compound stages will play a certain role in the nuclear reactions too. The pre-equilibrium emission model (7, 8) should be considered as a phenomenological description of such processes.

4. CODES FOR STATISTICAL MODEL CALCULATIONS

Combined pre-equilibrium plus compound models have been incorporated into many computer codes, the most popular of which are ALICE, GNASH, and the recently released EMPIRE and TALYS codes. We will discuss the main features of these codes, which are important for understanding some divergence between calculations, and represent a means of estimating the uncertainties of such calculations.

ALICE-91 and ALICE-IPPE

ALICE-91 is one of the late versions of the widely distributed ALICE code developed by Blann [33], and based on the hybrid pre-equilibrium model and Weisskopf-Ewing formulae. The hybrid model considers explicitly the transition rates for colliding particles instead of averaging over all n-exciton states. The corresponding relationship of the hybrid model may be written as follows:

$$\frac{d\sigma_{ab}}{de_b} = \sigma_c(e_a) \sum_{n=n_0}^{\bar{n}} \frac{X_b^n \rho_{n-1}(U_b)}{\rho_n(U_c)} \frac{\lambda_{con}(e_b)}{\lambda_{con}(e_b) + \lambda_+(e_b)} D_n de_b \ , \tag{29}$$

where X_b^n is the relative contribution of an emitted particle (proton or neutron) to the density of n-exciton states, λ_{con} is the rate of nucleon emission in the continuum, λ_+ is the competing rate for a transition after two-body collisions to more complex n+2-exciton states, and the factor D_n is a depletion factor which represents the fraction of the population surviving decay prior to reaching the n-exciton configuration. The summation term in Eq. (29) covers configurations from n_0 to equilibrium corresponding to the number of excitons $\bar{n} \approx 2gt$, where g is the single-particle density of nucleons and t is the temperature of the excited nucleus.

The continuum emission rate is determined by the common relationship:

$$\lambda_{con}(e) = \frac{g_s m e \sigma_c^*(e)}{\pi^2 \hbar^3 g} \ , \tag{30}$$

where all quantities are the same as in Eq. (2).

Blann has estimated the rate of transition to more complex states on the basis of nucleon mean-free-path calculations through the equation:

$$\lambda_+(e) = [1.4 \cdot 10^{21}(e + B_\nu) - 6.0 \cdot 10^{18}(e + B_\nu)^2] \quad \text{sec}^{-1}, \tag{31}$$

where B_ν is the nucleon (proton or neutron) binding energy in the nucleus and all energies are given in MeV.

Comparing Eqs. (29 - 31) with Eqs. (5) and (6), we can see that the main difference between the hybrid and standard pre-equilibrium models relates to the determination of the matrix elements responsible for the transition to more complex states. However, this difference has a relatively weak influence on the results of most calculations, because for both models the strength of the matrix element $|M|^2$ is adjusted to the available experimental data on spectra of emitted nucleons. Analysis of such data shows that λ_+ should be reduced by a factor of 5 relative to Eq. (31) to achieve an agreement of the hybrid model calculations with experimental data [10].

A more consistent consideration of the two-body collisions was obtained for the geometry dependent hybrid model [12], in which the dependence of the mean free path and the density of particle-hole excitations on the defuse distribution of nuclear matter in nuclei was taken into account. A much better description of the emitted nucleon spectra was achieved for this model.

The ALICE-91 code contains both versions of the hybrid model, although only the nucleon emission was included at the preequilibrium stage. α-particle and deuteron (or other light cluster) emissions are possible from the equilibrium compound stage solely. Gamma-ray emission from the compound nucleus was included to improve the description of the excitation functions for the charge-particle induced reactions at near threshold regions.
ALICE-91 uses two simple models for the level density of the compound nuclei: the standard Fermi-gas model with the corresponding pairing correction, or the back-shifted Fermi-gas model. There is also the option to include level density parameters from the Kataria and Ramamurthy prescription that simulate shell effects [34]. Calculations of the absorption cross sections by the optical model normally use the default parameters, which have been verified by the analysis of a large amount of experimental data [35].
The ALICE-IPPE code is the ALICE-91 version modified by the Obninsk group to include the pre-equilibrium cluster emission and the generalized superfluid model for the nuclear level densities [36]. An approach developed by Iwamoto and Harada [15] was used to simulate the cluster emission of α-particles, deuterons and tritons. The level density model includes both the energy-dependent shell effects and the corresponding collective enhancement of the level densities. ALICE-IPPE calculations use the same optical potential parameters for neutrons and protons as ALICE-91, but for α-particles and deuterons such parameters were slightly modified to reproduce the available experimental data on the absorption cross sections at low energies [37, 38].

GNASH
The GNASH code is based on the Hauser-Feshbach formalism plus the preequilibrium model with full angular momentum conservation. Calculations can be carried out with rather large schemes of low-lying discrete levels which is very important for neutron-induced reactions at low energies. A reasonably complete description of the current version of GNASH is given in Ref. [39]. This code has been used extensively by many people to produce evaluated data for national nuclear data libraries.
All particle transmission coefficients are introduced into the GNASH calculations from the external input file that is obtained from either the spherical or coupled-channel optical model. The code calculates the contribution of direct processes to the excitation functions by means of the introduction of additional input data.
Preequilibrium emission calculations can be undertaken by means of the PRECO-B code developed by Kalbach [40] and adopted in GNASH. Pre-equilibrium configurations are classified according to the number of particles and holes excited, and the exciton model involves solving a series of master equations that describe the equilibration of an excited nucleus through a series of two-body collisions producing more complex configurations of particle-hole pairs. The matrix element in expressions for the transition rates similar to Eq. (6) was parameterized in GNASH as the exciton-number dependent function:

$$
\begin{aligned}
M^2 &= \frac{k}{A^3 e}\sqrt{\frac{e}{7MeV}}\sqrt{\frac{e}{2MeV}} && \text{for e} < 2\ \text{MeV}\ , \\
&= \frac{k}{A^3 e}\sqrt{\frac{e}{7MeV}} && \text{for}\ \ 2 < \text{e} < 7\ \text{MeV}\ , \\
&= \frac{k}{A^3 e} && \text{for}\ \ 7 < \text{e} < 15\ \text{MeV}\ , \\
&= \frac{k}{A^3 e}\sqrt{\frac{15MeV}{e}} && \text{for e} > 15\ \text{MeV}\ ,
\end{aligned}
\qquad (32)
$$

where $e=U_c$ /n and U_c is expressed in MeV. The constant k is usually set equal to 130-160 MeV. The cluster preequilibrium emission was included on the basis of a phenomenological description by Kalbach [41].
The above preequilibrium model does not take into account angular momentum effects. Some simple approaches to estimate the spin populations of the residual nuclei following preequilibrium decay have been developed for GNASH. Three options are available for the population in the continuum region:

i) the calculated compound-nucleus spin distribution weighting of the preequilibrium cross-section components,
ii) pure level density spin distribution for the weighting, and
iii) the particle-hole spin distributions for the corresponding weighting.

Distributions of the pre-equilibrium components among the discrete levels are obtained by extrapolating the dependency of the preequilibrium cross-section energy to the nuclear level energies.

GNASH provides the user with three alternative models for the determination of the level density of compound nuclei: Gilbert-Cameron approach, back-shifted Fermi-gas model, Ignatyuk form of that Fermi-gas model that includes the energy-dependent shell effects. Parameters for each model can be adjusted automatically to the input data describing the density of the neutron resonances. A similar adjustment can be done for the gamma-ray widths.

The GNASH code used by the Obninsk group has been slightly modified to include the width fluctuation corrections of Eq. (3.3) omitted in the original version, and to add the collective enhancement into the description of the level density.

EMPIRE and TALYS

The EMPIRE code complex includes the largest set of nuclear reaction models used for a practical evaluation of nuclear data over a wide energy range, including the optical and direct reaction models, preequilibrium exciton model, and the full-featured Hauser-Feshbach-Moldauer model. A comprehensive paper on EMPIRE capabilities has recently been published in Ref. [42], and we refer interested readers to this work for the detailed technical information about the code.

The coupled-channel ECIS03 code [43] has been incorporated into EMPIRE-2.19 and was used for optical model calculations employing the individual potentials from the RIPL-3 database. Pre-equilibrium emission was taken into account by the PCROSS or HMS modules; the former features the one-component exciton model with gamma, nucleon and cluster emission (Iwamoto-Harada model), while the latter is an implementation of the Hybrid Monte-Carlo simulation approach to the pre-equilibrium emission of nucleons [44].

Among the various models describing level densities implemented in EMPIRE, the default calculations adopt that described as “EMPIRE specific”. This formalism uses the superfluid model below and the Fermi gas model above the critical excitation energy. Deformation-dependent collective effects on the level densities due to nuclear vibration and rotation (rotational and vibrational enhancements and their temperature-dependent damping) are taken into account. The shell corrections, pairing and asymptotic values of the level density parameter have been estimated using RIPL-2 recommendations. The corresponding systematics of the level density parameters was constructed of the basis of the experimental data on the neutron resonance densities. Values of the level density parameter at neutron binding energy $a(B_n)$ are compared against experimental data in Fig. 7. The systematics describes adequately the shell structure, but tends to underestimate scatter of the experimental points for the deformed nuclei, especially for the actinides.

The TALYS code complex is similar to EMPIRE in many respects and its main differences relate to simulation of the pre-equilibrium stage of nuclear reactions [45]. The two component description of the particle-hole excitations is used in TALYS, whereas a one-component formulation with a charge factor is used in EMPIRE. Some differences are available also in simulation of a cluster emission. Unfortunately, up to now it is difficultly to conclude which options of pre-equilibrium models are preferable for nuclear reaction analysis.

5. COMPARISON OF MODELLING RESULTS

The cross sections of ^{103}Rh(p,n)^{103}Pd and ^{103}Rh(d,2n)^{103}Pd reactions are shown in Figs. 8 and 9 in comparison with the available experimental data [18]. These calculations involve the use of the same optical potential and level density parameters for all reaction channels. The cross-sections calculated for the different codes agree reasonably well for the region, where the processes for the compound nucleus dominate; but for higher energies in which the contributions of the preequilibrium processes are rather large, significant discrepancies arise between the models. These

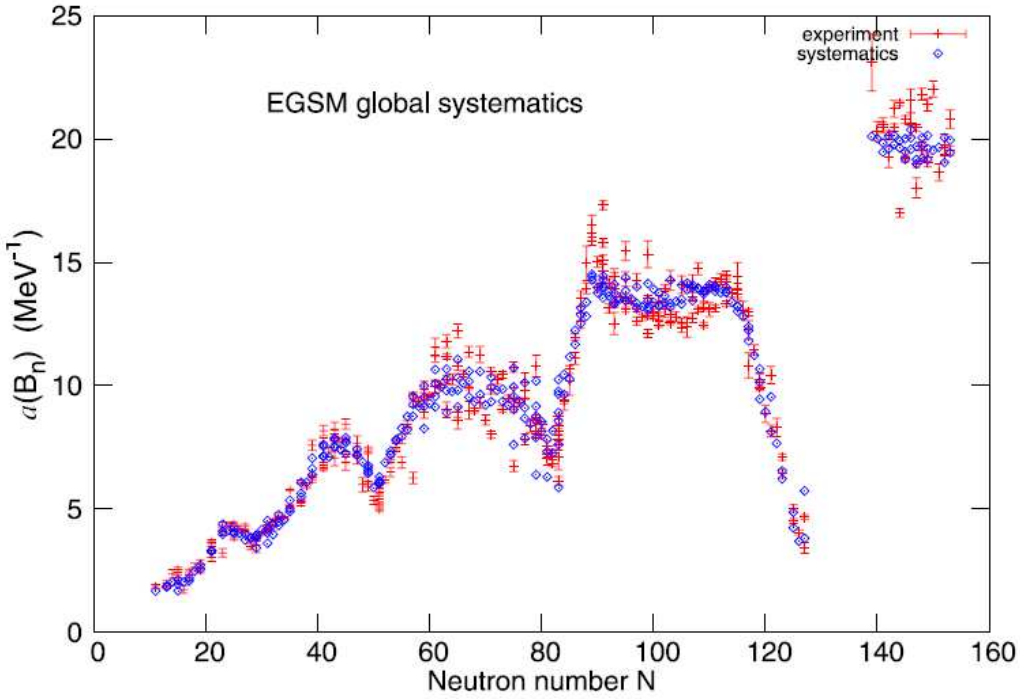

Fig. 7: Level density parameter $a(B_n)$ at the neutron binding energy. Predictions of the global systematics (blue squares) are compared with the experimental data (red points with error bars).

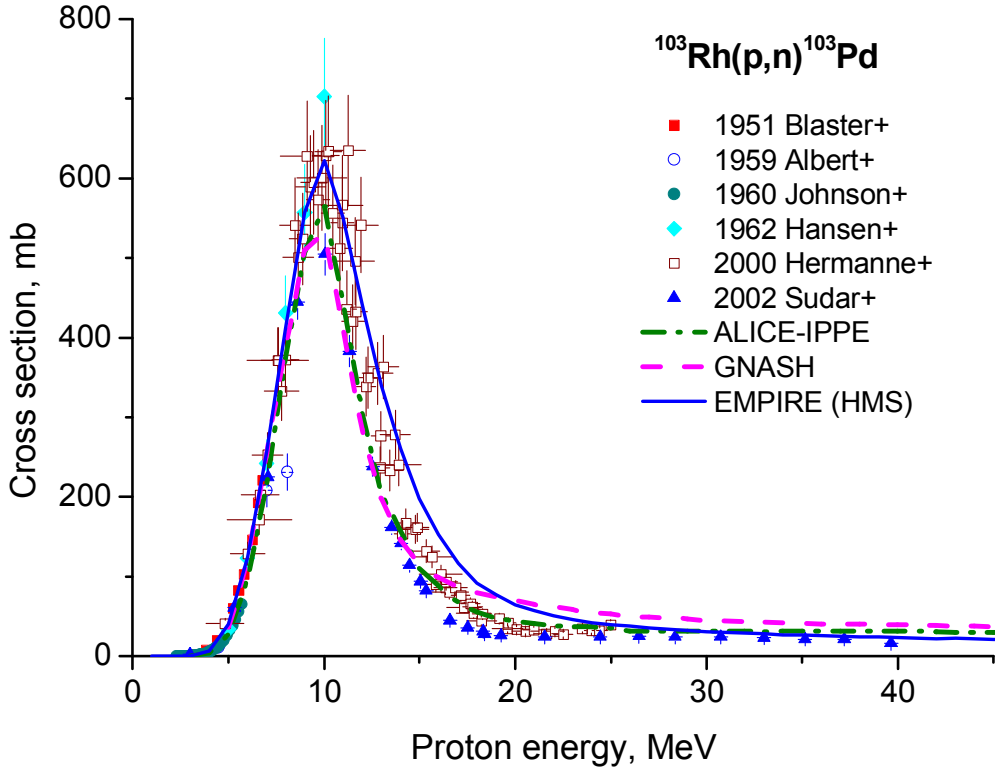

Fig. 8. Experimental data for the ^{103}Rh(p, n)^{103}Pd reaction cross-section in comparison with calculations by different codes.

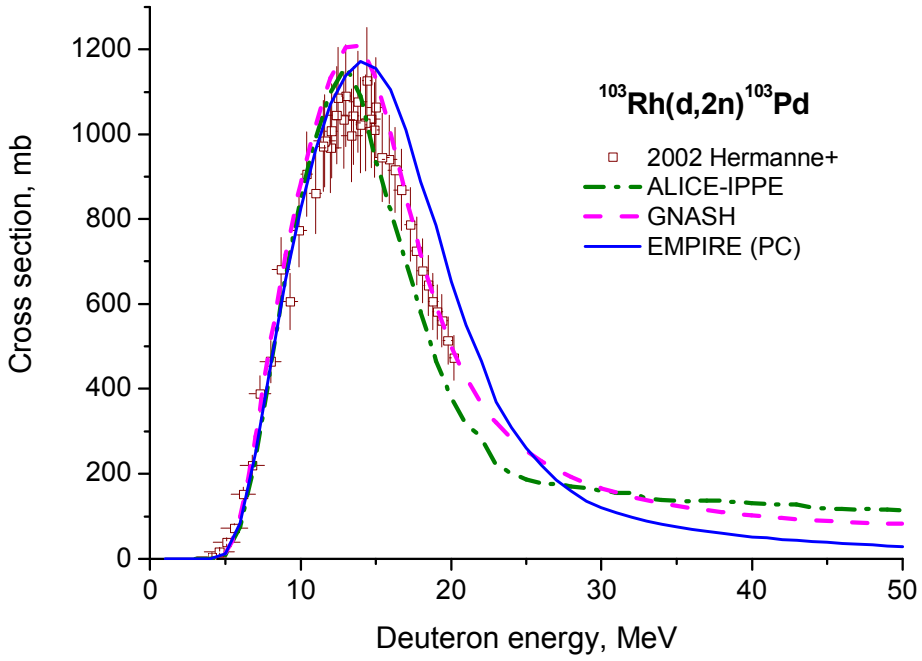

Fig. 9. Experimental data for the ^{103}Rh(d, 2n)^{103}Pd reaction cross-section in comparison with calculations by different codes.

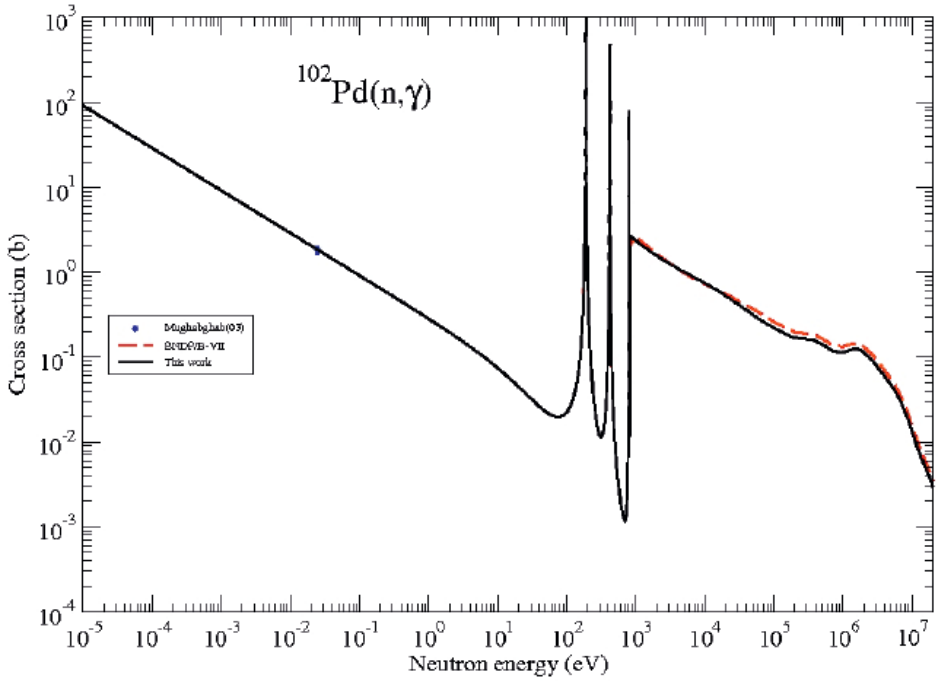

Fig. 10. ^{102}Pd(n, γ) capture cross-section for the production of ^{103}Pd.

discrepancies relate either to different parameterizations of the transition rates of Eq. (8), or to the corresponding matrix elements of the various codes (30, 31). The descriptions of the transition rate include some adjusted parameters in all codes, and uncertainties in these parameters are the main source of the resulting uncertainties of the calculated cross- sections.

Palladium-103 is a low energy X ray emitter used increasingly for brachytherapy. The $J^{\pi}= 5/2^{+}$ ground state decays exclusively by electron capture with a half-life of $T_{1/2}$ = 16.991(19) d. The Q-value for this decay mode is 543.1(8) keV, with an average light particle (electron) energy of 4.90(14) keV and an average gamma ray energy of 14.4(3) keV. The most recent version of the radioactive decay file can be found in the ENDF/B-VII library. The experimental values of the thermal capture cross-section and the capture resonance integral are given by Mughabghab [31]. The capture cross-section for the ^{102}Pd(n, γ)^{103}Pd reaction evaluated on the basis of statistical model calculations is shown in Fig. 10 [18]. There are no essential differences in various evaluations in spite of experimental data deficiency for the fast-neutron energy region.
Only some examples of the statistical model calculations for medical applications are considered in the present lecture. Much more such data are available in Ref. [18].

REFERENCES

1. BOHR, N., Neutron Capture and Nuclear Constitution, Nature **137** (1936) 344-348.
2. V.F. Weisskopf, D.H. Ewing, On the Yield of Nuclear Reactions with Heavy Elements, Phys. Rev. **57** (1940) 472-485.
3. W. Hauser, H. Feshbach, The Inelastic Scattering of Neutrons, Phys. Rev. **87** (1952) 366-373.
4. H. Feshbach, C.E. Porter, V.F. Weiskopf, Model for Nuclear Reactions with Neutrons, Phys. Rev. **96** (1954) 448-464.
5. P. Moldauer, Theory of average neutron reaction cross section in the resonance region, Phys. Rev. **123** (1961) 968-978.
6. N. Austern, Direct Nuclear Reaction Theories. Wiley-Interscience, New York, 1970
7. G.R. Satchler, Direct Nuclear Reactions, Clarendon, Oxford, 1983.
8. J.J Griffin, Statistical Model of Intermediate Structure, Phys. Rev. Lett. **17** (1966) 478-481.
9. F.C. Williams, Particle-hole State Density in the Uniform Spacing Model, Nucl. Phys. A **166** (1971) 231-240.
10. M. Blann,, Extensions of Griffin's Statistical Model for Medium-Energy Nuclear Reactions, Phys. Rev. Lett. **21** (1968) 1357-1360.
11. C.D. Harp, J.M. Miller, Precompound Decay from a Time-Dependent Point of View, Phys. Rev. C **3** (1971) 1847-1855.
12. M. Blann,, Hybrid Model for Pre-Equilibrium Decay in Nuclear Reactions, Phys. Rev. Lett. **27** (1971) 337-340.
13. E. Gadioli, E. Gadioli-Erba, P.G. Sona., Intermediate-state Decay Rates in the Exciton Model, Nucl. Phys. A **217** (1973) 589-610.
14. H. Feshbach,, A. Kerman, S. Koonin, Statistical Theory of Multi-step Compound and Direct Reactions, Ann. Phys. **125** (1980) 429-476.
15. A. Iwamoto, K. Harada, Mechanism of Cluster Emission in Nucleon-induced Preequilibrium Reactions, Phys. Rev. C **26** (1982) 1821–1834.
16. H. Nishioka, H.A. Weidenmuller, S. Yoshida, Statistical Theory of Precompound Reactions: The Multistep Direct Process, Ann. Phys. **183** (1988) 166-187.
17. E. Gadioli, P.E. Hodgson, Pre-equilibrium Nuclear Reactions, Clarendon Press, Oxford, 1992.
18. E. Betak, A.D. Caldeira, R. Capote, B.V. Carlson, Choi, H.D., Gumaraes, F.B., Ignatyuk, A.V., Kim, S.K., Kiraly, B., Kovalev, S.F., Menapace, E., Nichols, A.L., Nortier, M., Pompeia, P., Qaim, S.M., Scholten, B., Shubin, Yu.N., Sublet, J.-Ch., Tarkanyi, F., Nuclear Data for the Production of Therapeutic Radionuclides, Technical Report Series No 473, IAEA, Vienna, 2011.
19. H. Bethe, "Nuclear Physics B. Nuclear Dynamics, Theoretical",Rev. Mod. Phys. 9, 69-244 (1937).
20. T. Belgya, R. Capote, S. Goriely, M. Herman, S. Hilaire, A.V. Ignatyuk, A. Koning, V. Plujko, M. Avrigeanu, T. Fukahori, O. Iwamoto, M. Sin, E.S. Soukhovitskii, P. Talou and Y. Han, "Handbook for calculations of nuclear reaction data, Reference Input Parameter Library-3", IAEA Tech. Rep., International Atomic Energy Agency, Vienna, Austria, to be published (see http://www-nds.iaea.org/RIPL-3/).

21. P. Möller, J.R. Nix, W.D. Myers and W.J. Swiatecki, "Nuclear ground-state masses and deformations", At. Data Nucl. Data Tables 59, 185-381 (1995).
22. T. Ericson, "The statistical model and nuclear level densities", Adv. Phys. 9, 425-511 (1960).
23. A. Gilbert and A.G.W. Cameron, "A composite nuclear level density formula with shell corrections", Can. J. Phys. 43, 1446-1496 (1965).
24. W. Dilg, W. Schantl, H. Vonach and M. Uhl, "Level density parameters for the back-shifted Fermi gas model in the mass range 40 < A < 250", Nucl. Phys. A217, 269-298 (1973).
25. A.V. Ignatyuk, G.N. Smirenkin and A.S. Tishin, "Phenomenological description of the energy dependence of the level density parameter", Yad. Fiz. 21, 485-490 (1975) (in Russian).
26. A.V. Ignatyuk, "Statistical Properties of Excited Atomic Nuclei", Energoatomizdat, Moscow (1983) (in Russian); Rep. INDC(CCP)-233, International Atomic Energy Agency, Vienna, Austria, 1985.
27. A. Bohr and B. Mottelson, "Nuclear Structure", vol 2, Benjamin Inc., New York and Amsterdam (1974).
28. Fernbach H., Sorber R., Taylor T., The Scattering of High Energy Neutrons by Nuclei, Phys. Rev. **75** (1949) 1352.
29. Barschall, H., Regularities in the Total Cross Sections for Fast Neutrons, Phys. Rev. **86** (1952) 431
30. H. Feshbach, C.E. Porter, V.F. Weiskopf, Model for Nuclear Reactions with Neutrons, Phys. Rev. **96** (1954) 448-464.
31. S.F. Mughabghab, "Atlas of Neutron Resonances", Elsevier, Amsterdam - Tokio, 2006.
32. T. Tamura, "Analysis of the scattering of nuclear particles by collective nuclei in terms of the coupled-channel calculation", Rev. Mod. Phys. 37, 679-708 (1965).
33. BLANN, M., Recent Progress and Current Status of Preequilibrium Reaction Theories and Computer Code ALICE, Technical Report UCRL-JC-109052 (1991).
34. Kataria, S.K., Ramamurthy, V.S., Macroscopic Systematics of Nuclear Level Densities, Nucl. Phys. A **349** (1980) 10-28.
35. Blann, M., Vonach, H.K., Global Test of Modified Precompound Decay Models, Phys. Rev. C **28** (1983) 1475-1492.
36. Dityuk, A.I., Konobeyev, A.Yu., Lunev, V.P., Shubin, Yu.N., New Advanced Version of Computer Code ALICE – IPPE, Rep. INDC(CCP)-410, IAEA, Vienna (1998).
37. Auce, A., Carlson, A.R.F., Cox, A. J., Ingemarsson, A., Johansson, R., Renberg, P.U., Sundberg, O., Tibell, G., Reaction Cross-Sections for 38, 65, and 97 MeV Deuterons on Targets from ^{9}Be to ^{208}Pb, Phys. Rev. C **53** (1996) 2919-2925.
38. V. Avrigeanu, W. Oertzen, A.J.M. Plompen, Optical Model Potentials for Alpha-particles Scattering Around the Coulomb Barrier on A~100 Nuclei, Nucl. Phys. A **723** (2003) 104-126.
39. Young, P.G., Arthur, E.D., Chadwick, M.B., pp. 227-404 in Nuclear Reaction Data and Nuclear Reactors, A.GANDINI, G. REFFO (Eds), World. Sci., Singapore, 1996.
40. C. Kalbach, Multiple Preequilibrium Emission Code PRECO, Report CEN-DPh-N/BE/94/3, 1994.
41. C. Kalbach, The Griffin Model, Complex Particles and Direct Nuclear Reactions, Z. Phys. A **283** (1977) 401-411.
42. M. Herman, R Capote, B.V. Carlson, P. Oblozinsk.y, M. Sin, A. Trkov, H. Wiencke and V. Zerkin, EMPIRE: Nuclear Reaction Model Code System for Data Evaluation, Nucl. Data Sheets **108** (2007) 2657-2717.
43. J. Raynal,, Optical model and coupled-channels calculations in nuclear physics, p. 281 in Computing as a language of physics, ICTP International Seminar Course, Trieste, Italy, 2-10 August 1971, IAEA, Vienna (1972), J. Raynal, **ECIS** code, distributed by NEA DATA BANK, OECD, Paris.
44. M. Blann, "New precompound decay model," Phys. Rev., vol. C54, p. 1341, 1996.
45. A.J. Koning, S. Hilaire and M. Duijvestijn, "TALYS-1.0: A nuclear reaction program", User Manual, NRG/CEA, December 2007.